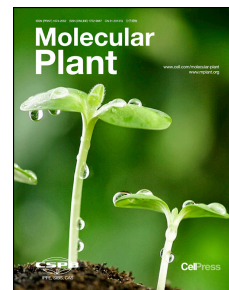# Accepted Manuscript

The cellulose synthases are cargo of the TPLATE adaptor complex

Clara Sánchez-Rodríguez, Yanyun Shi, Christopher Kesten, Dongmei Zhang, Gloria Sancho-Andrés, Alexander Ivakov, Edwin R. Lampugnani, Kamil Sklodowski, Masaru Fujimoto, Akihiko Nakano, Antony Bacic, Ian S. Wallace, Takashi Ueda, Daniel Van Damme, Yihua Zhou, Staffan Persson

Please cite this article as: **Sánchez-Rodríguez C., Shi Y., Kesten C., Zhang D., Sancho-Andrés G., Ivakov A., Lampugnani E.R., Sklodowski K., Fujimoto M., Nakano A., Bacic A., Wallace I.S., Ueda T., Van Damme D., Zhou Y., and Persson S.** (2018). The cellulose synthases are cargo of the TPLATE adaptor complex. Mol. Plant. doi: 10.1016/j.molp.2017.11.012.

This is a PDF file of an unedited manuscript that has been accepted for publication. As a service to our customers we are providing this early version of the manuscript. The manuscript will undergo copyediting, typesetting, and review of the resulting proof before it is published in its final form. Please note that during the production process errors may be discovered which could affect the content, and all legal disclaimers that apply to the journal pertain.

1   **Molecular Plant**

2   Letter to the Editor

3

4   **The cellulose synthases are cargo of the TPLATE adaptor complex**

5

6   Dear Editor,

7   Clathrin mediated endocytosis (CME) is an evolutionary conserved mechanism by which plasma

8   membrane (PM)-based cargo proteins are recognized by adaptor protein complexes and internalized.

9   Apart from the canonical adaptor complex, AP-2, plant cells rely on the TPLATE complex (TPC) to

10 execute CME (Gadeyne et al. 2014). The TPC is an octameric protein complex, consisting of

11 TPLATE, TASH3, LOLITA, TWD40-1, TWD40-2, TML, AtEH1 and AtEH2 (Gadeyne et al. 2014).

12 As the complex components are not conserved in yeast and animal cells CME initiation appears to be

13 regulated differently in plants (Hirst et al. 2014). This raises important evolutionary questions

14 concerning CME and cargo recognition across eukaryotic Kingdoms (Zhang et al. 2015). Based on *in*

15 *silico* analysis TASH3, TPLATE, TML and LOLITA might have functions related to AP-2A, AP-2B,

16 AP-2M and AP-2S, respectively (Hirst et al 2014; Zhang et al. 2015), which may include cargo

17 recognition and clathrin recruitment to the PM. Indeed, similar to Arabidopsis AP2M and AP2S (Fan

18 et al. 2013), TPLATE and TML are required for clathrin recruitment to the PM, even after AP-2

19 depletion (Wang et al. 2016). Therefore, we hypothesized that these proteins are involved in cargo

20 recognition in plants.

21 Loss of TPC function results in male sterility (Gadeyne et al. 2014), similar to loss-of-function

22 mutants of cellulose synthesis (Persson et al. 2007). CME has been reported to mediate cellulose

23 synthase (CESA) complexes (CSCs) internalization in elongating hypocotyl cells (Bashline et al.,

24 2013, 2015); supported by live cell imaging data (Supplemental Figure 1; (Miart et al. 2014). Since

25 cellulose synthesis is essential for plant growth and the CSCs are unique to plants, it might be

26 expected that the CESAs are TPC cargo, which could explain why the TPC is maintained in plants

27 but not in animals and yeasts. To test this, we performed co-immunoprecipitation (Co-IP)

28 experiments, which revealed that CESA6, a component of the primary wall CSC, interacts with both

29 TML and TPLATE (Figure 1A, upper panel). We corroborated this finding by bimolecular

1

30   fluorescence complementation (BiFC) between the Arabidopsis primary wall CESAs, i.e. CESA1, 3

31   and 6 and TPLATE (Figure 1A bottom panel and Supplemental Figure 2). To confirm that the

32   detected fluorescent signals were not due to either over-expression or random collisions of the split

33   FP halves, we co-expressed each of the primary CESAs with AtEH1, another subunit of the TPC.

34   Here, we did not observe any detectable fluorescent signal from the BiFC assays (Figure 1A bottom

35   panel and Supplemental Figure 2A and C), confirming that the TPLATE-CESA interactions are

36   specific in our BiFC system and suggesting a lack of direct interaction between AtEH1 and the

37   CESAs, while being connected through TPLATE. Notably, the CESA-TPLATE interactions

38   correlated with a change in CESA localization patterns; from a homogeneous and diffuse distribution

39   to a speckled pattern (Figure 1A bottom panel and Supplemental Figure 2A), possibly indicating

40   internalized CSCs. To test this hypothesis, we repeated the BiFC assay between CESA6 and

41   TPLATE in the presence of the clathrin marker CLC2-mCh (Supplemental Figure 2B and D). Here,

42   the BiFC signal of the CESA-TPLATE co-localized with the clathrin marker CLC2-mCh

43   (Supplemental Figure 2B). As expected from the multiple roles of clathrin, we also observed

44   mCherry fluorescence at cellular compartments not marked by TPLATE-CESA interactions.

45   Defects in CESA internalization are likely to result in severe cellulose deficiency. Accordingly, lines

46   altered in *TML* expression, pESTR:*amiR-TML* (Gadeyne et al. 2014)*,* displayed defects in hypocotyl

47   and root elongation (Figures 1B-upper panels), concomitant with cell swelling (Supplemental Figure

48   3C), similar to what is found in seedlings impaired in primary wall cellulose synthesis (McFarlane et

49   al. 2014). Furthermore, we observed a strong reduction in cellulose content and an increase in sugars

50   corresponding to non-cellulosic polysaccharides, mainly those of pectin-related monosaccharides

51   (e.g. uronic acids) compared to control seedlings (Figures 1B-bottom panel and Table S1). Plants

52   impaired in two other main steps of CME: vesicle assembly by clathrin triskelia

53   (pINTAM>>RFP-HUB) and vesicle scission (*drp1a-2/rsw9-2*), showed similar phenotypes and cell

54   wall composition to the *amiR*:*TML* line (Supplemental Figure 3 and Table S1). Interestingly, a null

55   mutant for a subunit of the other plant early adaptor complex, the canonical AP-2 (*ap2m-1*), showed

56   increase in hypocotyl length, did not display defects in cell swelling and its sugar composition was

57   comparable to wild-type seedlings (Supplemental Figure 3, Table S1; Bashline et al., 2015).

58   Defects in CESA internalization should impact CESA dynamics at the PM. Live cell imaging

2

59 revealed an increase in FP-CESA6 density at the PM in *amiR*-TML seedlings compared to their

60 control (0.9 ± 0.1 foci/µm^2 in control cells versus 1.6 ± 0.1 foci/µm^2 in *amiR-TML* cells; Figure 1C left

61 and upper-right panels). The increase in FP-CESA6 density could be due to either an enhanced

62 delivery or a reduced internalization rate of the CSCs to and from the PM, respectively. To differentiate

63 between these processes, we calculated the CESA delivery rate (Gutierrez et al. 2009), and found no

64 differences in CESA delivery rate to the PM between the lines (Figure 1C upper-right panel). The

65 increased CESA6 density at the PM should therefore reflect a reduction in the internalization rate of

66 CSC when TML activity is impaired. Moreover, the reduction of CESA6 internalization correlated

67 with an increased amount of slow moving CESA particles at the PM (indicated by less tilted traces in

68 kymographs; Figure 1C left panel). The *drp1a-2* mutant showed similar CSC homeostasis at the PM

69 as observed for *amiR-TML*; i.e., increased CESA6 density and slow-moving particles (Supplemental

70 Figure 4). As CESA movement is related to its activity this explains the reduced cellulose content in

71 the TML and DRP1A knockdown/knock-out lines. As reported previously (Bashline et al., 2015), we

72 did not observe any differences in the CSC speed at the PM between *ap2m-1* and wild-type cells

73 (Supplemental Figure 4) and nor did we observe any significant differences in FP-CESA6 density at

74 the PM in *ap2m-1* as compared to wild-type (Supplemental Figure 4B). While these data contrast with

75 previous reports (Bashline et al. 2013; 2015), they do explain the absence of cellulose and anisotropic

76 cell growth reduction in the *ap2m-1* mutant as compared to the wild-type (Supplemental Figure 4;

77 Bashline et al., 2015). Our results therefore indicate that the TPC is key in the regulation of CSC

78 trafficking and, hence, cellulose synthesis in Arabidopsis seedlings.

79 With the aim of exploring whether CESAs are also internalized via TPC-related CME in other plant

80 species, we performed split-Luciferase assays combining the rice TPC proteins *Os*TML and

81 *Os*TPLATE2, with *Os*CESA8 and *Os*CESA4, which are primary and secondary wall rice CESAs,

82 respectively. We could detect clear luciferase signals from these assays, which indicate that the rice

83 CSCs also interact with TPC components (Figure 1D). In addition, we performed

84 immuno-precipitation (IP) using an *Os*CESA4 antibody coupled with mass spectrometry (MS) to

85 identify *Os*CESA4 interactors in rice plants. Notably, we found several TPC subunits, including

86 *Os*TPLATE2, *Os*TML, *Os*TWD40-1, *Os*EH2, *Os*TASH3, and *Os*DRP2B/BC3, as well as other

87 cellulose-related proteins in the pellet (Table S2). Our mass spec results did not identify AP-2

88 subunits in the pull-downs of any of our IP replicates. Hence, CSCs might also be CME cargo

89 recruited by the TPC early adaptor in rice.

90 *In vivo* evidence for cargo-CME co-internalization, and re-localization of cargo by the CME

91 components via BiFC, has not been reported in plants. In addition, we were able to identify a plant

92 CME cargo by IP-MS, which is rare in plant biology. Hence, our results provide a foundation for

93 further elaborations of CME-mediated events in plant cells. Our *in vivo* interaction data between

94 TPLATE and TML with CSC, both in Arabidopsis and rice, indicate that TPLATE and TML might

95 recognize the CSC for its internalization. TML has a muHD domain that is also present in APμ

96 subunits (e.g. AP-2M in the AP-2 complex) and in the muniscins (Hirst et al. 2014; Zhang et al.

97 2015), so it might be anticipated that TML can recognize cargo. Notably, some protein domains

98 suggest a relationship between TPLATE and AP-2B, which does not include any cargo-recognition

99 motif. Our *in vivo* interaction results between TPLATE and CSC suggest that the TPLATE subunit of

100 the TPC may have a cargo-binding capacity in plant cells.

101 Our results indicate that the TPC is the main early adaptor that recognizes CSC for its internalization

102 via clathrin. The data presented in the current work are in agreement with the fact that the TWD40-2

103 subunit of the TPC contributes to cellulose synthesis (Bashline et al. 2015), supporting a prominent

104 role of the TPC in this process. AP2-M has been shown to bind to the central cytosolic domain of the

105 primary CESAs (Bashline et al. 2013), which contain putative AP-2M binding domains (YxxΦ) in a

106 yeast assay. Therefore, the CSC might be recognized by both plant TPC and AP-2 early adaptors,

107 possibly at different regions of its cytosolic domains. Notably, TPC and AP-2 co-localize in

108 approximately 50% of all CME events, suggesting a complementary role of these CME adaptors

109 (Gadeyne et al. 2014), plausibly relating to particular cargo or certain growth circumstances. This

110 might be the case under certain stress conditions, such as those experienced by the plant when the

111 TPC is not fully active (Barth and Holstein 2004; Bashline et al. 2015).

112 In summary, although it has been shown that several cargo proteins showed defective internalization

113 upon depletion of TPC subunits (Gadeyne et al., 2014), our data represent the CSC as the first

114 identified TPC-cargo interaction in seed plants, recognized by TML and TPLATE subunits, adding

115 insights into the evolution of cargo recognition in plant CME.

116

117   **Figure Legend**

118   **Figure 1. TPLATE and TML interact with CESAs and influence cellulose synthesis**

119   **A. Arabidopsis primary wall CESAs interact with TML and TPLATE *in planta*.** (**Upper panel**)

120   Co-immunoprecipitation (Co-IP) shows that CESA6 interacts with the TPC subunits. (**Upper-left**) 10

121   µL of total extract of proteins Input (I), Non-bound (Nb) and Bound (B) fractions. (**Upper-right**) 25

122   µL of Bound fractions. The experiment was performed twice with similar results. (**Bottom panel**)

123   Bimolecular Fluorescence Complementation (BiFC) assays showing interaction of Arabidopsis

124   primary wall CESAs and TPC subunits in *N. benthamiana* epidermal leaf cells. The N-terminal (YN)

125   or C-terminal (YC) part of VENUS was fused in frame with CESA6, TPLATE and *At*EH1. Construct

126   combinations are indicated in each figure panel. As a transformation control, the nuclear marker

127   CFP-N7 (cyan) was included in all experiments.

128   **B. TML is essential for cell elongation and cellulose synthesis in Arabidopsis.   (Upper-left**

129   **panel)** Representative images of 5-day-old etiolated seedlings expressing pESTR:*amiR-TML*

130   (*amiR-TML*) and their control grown on either EtOH- or on 5 µM beta-estradiol (in

131   EtOH)-containing medium. Scale bars= 1cm. (**Upper-right panel**) Hypocotyl length of lines shown

132   in (Upper left). Data represent the average (±SE) of $n = 3$ biological replicates, each containing

133   20-30 seedlings. (**Bottom panel**) Cellulose and uronic acid (UA) content of the lines shown in

134   (Upper panels), represented as µg of glucose (D-Glc) or µg of glucuronic acid (GlcA) per mg of

135   dried alcohol insoluble residue (AIR), respectively. Data represent the average (±SE) of $n = 3$

136   biological replicates, each with three technical repetitions. Student's *t* test; P-value **<0.01, *< 0.05.

137   **C**. **Impaired TML function alters the density and dynamics of plasma membrane localized**

138   **CESAs. (Left panel)** Representative images from movies obtained with a spinning disk confocal

139   microscope of tdTomato-CESA6 in *amiR-TML* background and its control at the plasmam membrane

140   (PM) in hypocotyl cells of 3-day-old etiolated seedlings. PM particle density shown in single-frame

141   images (particles highlighted in magenta). Time averaged projections of frames acquired over 5 min,

142   and corresponding kymographs showing CESA6 trajectories and movement, respectively. Scale bars=

143   5µm. (**Upper-right panels**) Quantification of tdTomato-CESA6 density and delivery rate at the PM

144   in photo-bleached areas of cells imaged with a spinning disk confocal microscope. Data represent

145   average (±SE) of at least 6 cells per treatment or genotype; Student's *t* test P-value *<0.05; **<0.01.

146   (**Bottom-right panel**) Histogram of CSC speeds at the PM in tdTomato-CESA6 expressing seedlings

5

147 shown in (Left panel). Mean (±SE) speeds for each line or treatment are given in parentheses. $n \geq$

148 589 particles; $\geq$ 6 cells and $\geq$ 6 seedlings were tracked. A graph showing the percentage of slow

149 (0-200nm/min) and fast (>200nm/min) moving CSC is included in each panel.

150 **D. Rice primary and secondary wall CESAs can interact with TML and TPLATE2 *in planta*.**

151 Split-luciferase complementation assay showing that the primary cell wall *Os*CESA8 can interact with

152 *Os*TML (**Upper panel**) and *Os*TPLATE2 (**Middle panel**). The secondary wall *Os*CESA4 can interact

153 with *Os*TML (**Bottom panel**). Scale bars = 1cm

154

163

164 **Author contributions**

165 CSR, YZ and SP managed the project and wrote the article; CSR, YS, CK, DZ, GSA, LT, AI, ERL,

166 and MF carried out experiments; CSR, YZ, SP, AN, AB, and TU acquired funding and provided

167 supervision; KS, IW and DVD provided additional data; CSR, SP, DVD and AB reviewed and edited

168 the manuscript.   .

169

176

177 **Supplemental Information**

178 Document S1. Materials and Methods. Supplemental Figures 1-4, Supplemental Tables 1-3, and

179 Supplemental References.

180

181 **Clara Sánchez-Rodríguez[1,2*], Yanyun Shi[3], Christopher Kesten[1,2,4], Dongmei Zhang[3],**

182 **Gloria Sancho-Andrés[2], Alexander Ivakov[1,4,5], Edwin R. Lampugnani[4], Kamil**

183 **Sklodowski[2], Masaru Fujimoto[6‡], Akihiko Nakano[6,7], Antony Bacic[8], Ian S. Wallace[9],**

184 **Takashi Ueda[10], Daniel Van Damme[11,12], Yihua Zhou[3], Staffan Persson[1,4]**

185

186 [1]Max-Planck-Institute for Molecular Plant Physiology, Am Muehlenberg 1, 14476 Potsdam,

187 Germany

188 [2]Department of Biology, ETH Zurich, 8092 Zurich, Switzerland

189 [3]State Key Laboratory of Plant Genomics, Institute of Genetics and Developmental Biology, Chinese

190 Academy of Sciences, Beijing 100101, China

191 [4]School of Biosciences, University of Melbourne, Parkville 3010, Victoria, Australia.

192 [5]ARC Centre of Excellence for Translational Photosynthesis, Research School of Biology, Australian

193 National University, GPO Box 475, Canberra, ACT, 2601 Australia

194 [6]Department of Biological Sciences, Graduate School of Science, The University of Tokyo, Hongo,

195 Bunkyo-ku, Tokyo 113-0033, Japan.

196 [7]Live Cell Super-resolution Imaging Research Team, RIKEN Center for Advances Photonics,

197 Hirosawa, Wako, Saitama 351-0198, Japan.

198 [8]ARC Centre of Excellence in Plant Cell Walls, School of Biosciences, University of Melbourne,

199 Parkville 3010, Victoria, Australia.

200 [9]Department of Biochemistry and Molecular Biology, University of Nevada, Reno, NV, 89557

201 [10]Division of Cellular Dynamics, National Institute for Basic Biology, Okazaki, Aichi 444-8585, Japan

202 [11]Department of Plant Biotechnology and Bioinformatics, Ghent University, B-9052 Gent, Belgium

203 [12]Center for Plant Systems Biology, VIB, Technologiepark 927, B-9052 Gent, Belgium

204 [‡] Present address: Laboratory of Plant Molecular Genetics, Graduate School of Agricultural and

205 Life Sciences, The University of Tokyo, 1-1-1 Yayoi, Bunkyo-ku, Tokyo 113-8657, Japan.

206

207 *Correspondence: Clara Sánchez-Rodríguez (clara_sanchez@ethz.ch)

208

References

210 Barth M, Holstein SE (2004) Identification and functional characterization of Arabidopsis AP180, a
211 binding partner of plant alphaC-adaptin. Journal of Cell Science 117: 2051-2062

212 Bashline L, Li S, Anderson CT, Lei L, Gu Y (2013) The endocytosis of cellulose synthase in
213 Arabidopsis is dependent on *mu2*, a clathrin-mediated endocytosis adaptin. Plant Physiology 163:
214 150-160

215 Bashline L, Li S, Zhu X, Gu Y (2015) The TWD40-2 protein and the AP2 complex cooperate in the
216 clathrin-mediated endocytosis of cellulose synthase to regulate cellulose biosynthesis. Proceedings of
217 the National Academy of Sciences of the United States of America 112: 12870-12875

218 Fan L, Hao H, Xue Y, Zhang L, Song K, Ding Z, Botella MA, Wang H, Lin J (2013) Dynamic
219 analysis of Arabidopsis AP2 sigma subunit reveals a key role in clathrin-mediated endocytosis and
220 plant development. Development 140: 3826-3837

221 Gadeyne A, Sanchez-Rodriguez C, Vanneste S, Di Rubbo S, Zauber H, Vanneste K, Van Leene J, De
222 Winne N, Eeckhout D, Persiau G, Van De Slijke E, Cannoot B, Vercruysse L, Mayers JR,
223 Adamowski M, Kania U, Ehrlich M, Schweighofer A, Ketelaar T, Maere S, Bednarek SY, Friml J,
224 Gevaert K, Witters E, Russinova E, Persson S, De Jaeger G, Van Damme D (2014) The TPLATE
225 adaptor complex drives clathrin-mediated endocytosis in plants. Cell 156: 691-704

226 Gutierrez R, Lindeboom JJ, Paredez AR, Emons AM, Ehrhardt DW (2009) Arabidopsis cortical
227 microtubules position cellulose synthase delivery to the plasma membrane and interact with cellulose
228 synthase trafficking compartments. Nature Cell Biology 11: 797-806

229 Hirst J, Schlacht A, Norcott JP, Traynor D, Bloomfield G, Antrobus R, Kay RR, Dacks JB, Robinson
230 MS (2014) Characterization of TSET, an ancient and widespread membrane trafficking complex.
231 eLife 3: e02866

232 McFarlane HE, Doring A, Persson S (2014) The cell biology of cellulose synthesis. Annual Review
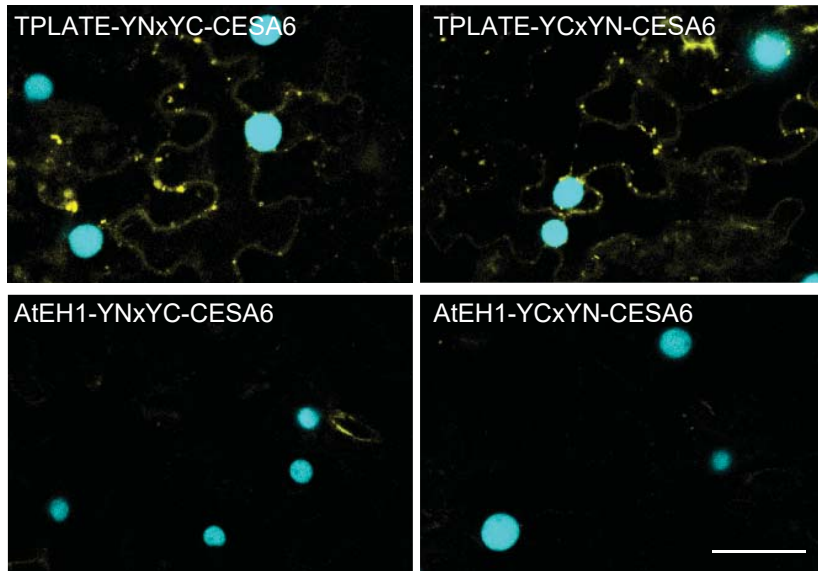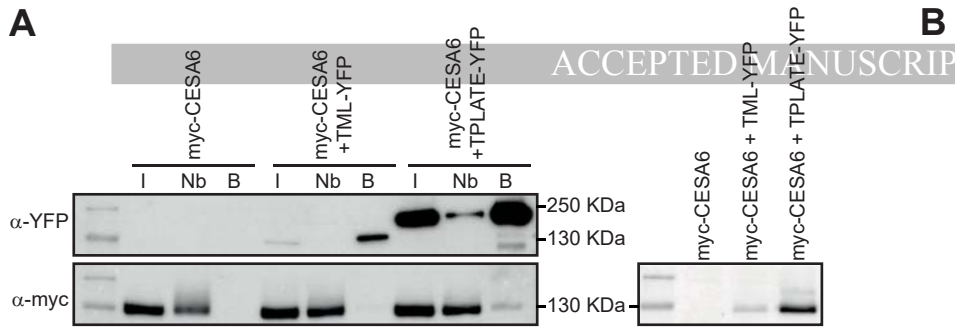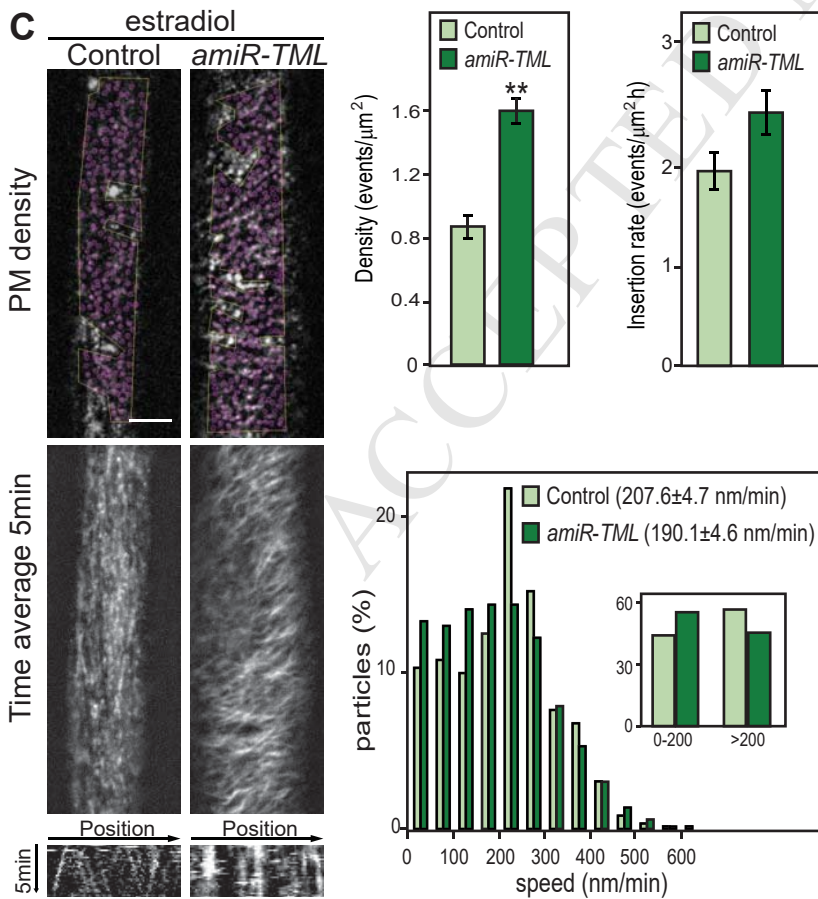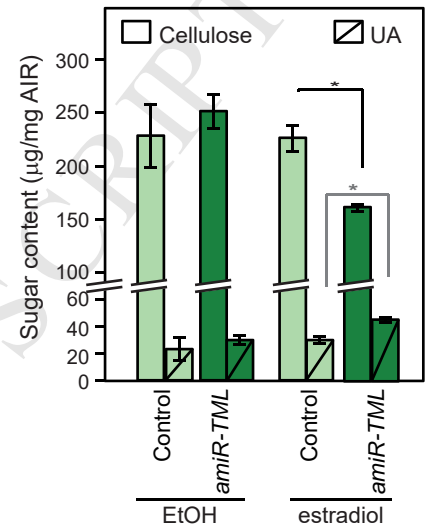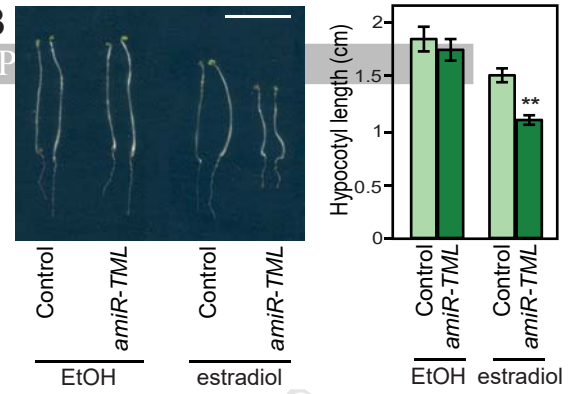233 of Plant Biology 65: 69-94

234 Miart F, Desprez T, Biot E, Morin H, Belcram K, Hofte H, Gonneau M, Vernhettes S (2014)
235 Spatio-temporal analysis of cellulose synthesis during cell plate formation in Arabidopsis. The Plant
236 Journal 77: 71-84

237 Persson S, Paredez A, Carroll A, Palsdottir H, Doblin M, Poindexter P, Khitrov N, Auer M,
238 Somerville CR (2007) Genetic evidence for three unique components in primary cell-wall cellulose
239 synthase complexes in Arabidopsis. Proceedings of the National Academy of Sciences of the United
240 States of America 104: 15566-15571

241 Wang C, Hu T, Yan X, Meng T, Wang Y, Wang Q, Zhang X, Gu Y, Sanchez-Rodriguez C, Gadeyne A,
242 Lin J, Persson S, Van Damme D, Li C, Bednarek SY, Pan J (2016) Differential regulation of clathrin
243 and its adaptor proteins during membrane recruitment for endocytosis. Plant Physiology 171:
244 215-229

245 Zhang Y, Persson S, Hirst J, Robinson MS, van Damme D, Sanchez-Rodriguez C (2015) Change

246 your TPLATE, change your fate: plant CME and beyond. Trends in Plant Science 20: 41-48